Catalysis Letters Vol. 110, Nos. 1–2, August 2006 (© 2006)
DOI: 10.1007/s10562-006-0102-2

The effect of exothermic reactions during regeneration on the NO_X trapping efficiency of a NO_X storage/reduction catalyst

William S. Epling,[a,*] Aleksey Yezerets,[b] and Neal W. Currier[b]

[a]*Department of Chemical Engineering, University of Waterloo, 200, University Ave West, Waterloo, Ontario N2L 3G1, Canada*
[b]*Cummins, Inc, MC 50183, 1900, McKinley Ave, Columbus, IN 47201, USA*

Received 31 March 2006; accepted 18 May 2006

An unusual behavior was observed during experiments conducted at 371 and 465 °C with a commercial NO_X storage/reduction catalyst: the outlet NO_X concentration during the trapping phase reached a cycle minimum after regeneration, increased for 20–30 s, as expected, but then surprisingly decreased, indicating the catalyst had become more efficient in trapping the entering NO_X. The results reported in this letter indicate that this phenomenon was caused by a superposition of two factors: a substantial exotherm associated with the regeneration event from reductant reacting with surface oxygen species and a negative impact of an evolving temperature profile on the dynamic NO_X storage capacity.

KEY WORDS: NO_X storage; NO_X reduction; diesel emissions.

1. Introduction

The use of diesel engines in passenger vehicles is expected to increase relative to gasoline engines. Coincidentally, upcoming environmental policy throughout most of the world is imposing requirements for significant decreases in tailpipe NO_X, hydrocarbon, CO and particulate emissions from diesel engines. To meet these challenges, new technologies are being developed, an example of which is NO_X storage/reduction (NSR) catalysis. NSR technology uses a cyclic process where NO_X is stored on a catalyst, ultimately as nitrates, under the normally-lean engine operating conditions. At some level of catalyst saturation, determined by the control strategy or needed reduction levels, the exhaust gas composition is forced rich in reductant relative to O_2, termed regeneration, and the trapped NO_X is released and non-selectively reduced to N_2. With the decomposition of the nitrates and release and reduction of NO_X, the trapping ability of the catalyst is thus restored. Five steps have been decoupled to describe this cyclic process [1]:

- NO oxidation,
- NO_2/NO sorption with nitrate formation,
- reductant evolution,
- NO_X release,
- and finally NO_X reduction to N_2.

The first two are associated with normal, lean-engine operation and the last three are associated with the induced rich/regeneration event. In vehicular applications, the trapping or lean-phase is typically on the order of > 1 min while the regeneration or rich-phase is on the order of a few seconds. NSR catalysts are typically composed of a strong basic component for the NO_X trapping and nitrate formation process, Ba being the most common in the literature, and a precious metal component to accommodate the multiple redox reactions that occur.

Decoupling these five steps is non-trivial as each step is dependent on the others. In practice, if one step fails, the catalyst fails. Various models have been developed describing the trapping process and coupling the first two steps [2–5]. This is necessary since one of the trapping mechanisms in nitrate formation is the disproportionation mechanism; $3NO_2 + BaO \rightarrow NO + 2Ba(NO_3)_2$. The product NO can then be re-oxidized to reactant NO_2 downstream of the trapping or nitrate formation site, which therefore keeps trapping and oxidation coupled [6]. The trapping reaction with nitrate formation is dependent on several parameters including temperature, gas composition and the extent of the preceding regeneration event. Previous research has demonstrated that the total amount of NO_X that can be trapped, using NO_2 as the reactant, decreases with temperature and the rate of trapping increases with temperature [1]. The extent of NO oxidation goes through a maximum with temperature due to coupled kinetic and equilibrium limitations [7–9]. These findings originated from tests with self-consistent gas compositions and samples that had been well regenerated, in theory removing all nitrates before the tests began. These results therefore demonstrate clear temperature dependencies.

*To whom correspondence should be addressed.

During application, there are of course no imposed delays between the rich- and lean-events and they therefore influence each other. During the rich-phase, the gas composition contains excess reductant in relation to any O_2 that is present. Nitrates decompose to NO_X, which is then reduced to N_2 by the excess reductant. At the interface between the rich-to-lean transition, there will be mixing of the reductant-rich and O_2-rich-phases resulting in exothermic reactions along the catalyst surface. Furthermore, any oxygen-storage-capacity (OSC) of the catalyst sample will also result in reaction between the introduced reductant and oxygen. The temperature of the catalyst can increase due to these two processes and unless this temperature dissipates at the same rate as the linear gas velocity through the catalyst, residual heat could influence the subsequent trapping phase reactions due to their temperature dependency. The data presented as part of this paper clearly show this phenomenon and indicate it must be taken into account when developing models of NSR systems.

2. Experimental

A commercial NSR catalyst formulation, manufactured by Umicore, was supplied via the Crosscut Lean Exhaust Emissions Reduction Simulations (CLEERS) group. Details of the formulation are emerging but are not presented as part of this work. The catalyst, 3″ length and 7/8″ diameter, was wrapped in insulation material and set in a quartz-tube reactor. The insulation material eliminates gas bypass between the catalyst and reactor wall. This reactor was then placed in a tube furnace. The dry gas mixtures were introduced using MKS Instruments mass-flow controllers. A four-way valve controlled the choice of lean or rich-phase introduction to the reactor. Water was introduced downstream of the valve in a heated zone upstream of the furnace. The trapping (or lean) mixture consisted of 5% H_2O, 5% CO_2, 10% O_2, 300 ppm NO and a balance of N_2. The reductant-containing or rich-phase contained 5% H_2O, 5% CO_2, 1.125% CO, 0.675% H_2 and a balance of N_2. The lean-phase was set for 60 s and the rich-phase for 5 s. Thirty lean/rich cycles were run at each test temperature. Both flowrates were set to establish a gas hourly space velocity of 30,000 h^{-1}. The amount of reductant added during the 5 s rich-phase corresponds to 2X the amount of reductant needed to reduce the integral amount of NO_X that entered during the trapping phase of the cycle. In other words, if all the entering NO_X was trapped, then twice the amount of reductant needed to reduce the nitrates to N_2 was added. If not all of the NO_X was trapped, then more than twice the needed amount of reductant was added. Prior to the cycling tests, the sample was heated to 550 °C and exposed to 5% H_2O, 5% CO_2, 1% H_2 and a balance of N_2 for 15 min. The sample was then cooled to the test temperature in 5% H_2O, 5% CO_2, 10% O_2 and a balance of N_2. All of these specifications are part of a proposed NSR catalyst test methodology designed by the CLEERS group. The cycling portion of the test was not started until all measured temperatures had been stable for at least 5 min. Gas analysis was conducted with universal exhaust gas oxygen (UEGO) sensors and a MKS MultiGas 2030 FTIR instrument, collecting data at a rate of $\sim$ 2 Hz. The gas was not dried prior to analysis. NO, NO_2, N_2O, NH_3, CO, CO_2 and H_2O were monitored throughout each experiment. Since the focus of this paper is the effects of the regeneration-induced exotherm on the trapping phase, the only N species presented are NO and NO_2 as none of the others were observed during the lean-phase of the cycles.

Thermocouples were placed in the radial center of the reactor tube just upstream and downstream of the catalyst, $\sim$2 mm away from the sample on each side. Also, a 0.020″ thermocouple was set just inside one of the radially central channels of the inlet face and one was set just inside one of the channels of the outlet face. A more accurate position cannot be given as the thermocouple tip cannot be seen inside the channel, however, they appear to be within 1–3 mm of the catalyst faces. These four were continuously monitored. In describing the data in the sections below, the temperatures that are listed for each test were recorded just prior to cycling from the thermocouple placed just inside the catalyst outlet face.

3. Results and discussion

The experiments consisted of 30 lean/rich cycles at each temperature. The NO slip data shown in figure 1 were obtained toward the end of the 30-cycle sets. At this stage of each experiment, there were no cycle-to-cycle variations in performance, whereas in the first several cycles significant performance changes were

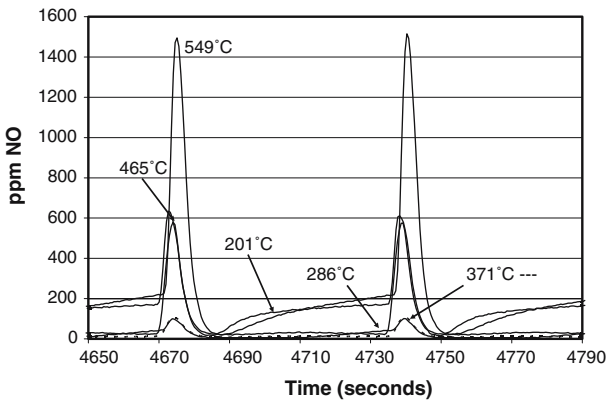

Figure 1. NO outlet concentrations toward the end of a 30-cycle test at 201, 286, 371, 465 and 549 °C. The gas concentrations are listed in the section 2.

observed. The NO_2 slip data are shown in figure 2 for the same cycles as those in figure 1. These two data sets show the typical, representative trends of NSR catalyst temperature dependence. Large NO_X releases during the regeneration phase and little trapping during the lean-phase occur with high-temperature operation. The actual NO_X to N_2 removal efficiency over the 30 cycles at 549 °C is 9%. At these temperatures, the surface nitrate species are unstable which results in the poor ability of the catalyst to store NO_X and form nitrate. Due to the weak stability of the nitrate species, a significant release of NO_X is noted at the beginning of the regeneration phase as the rate of release of NO_X that was stored at this high temperature overwhelms the reduction mechanism or rate. More NO_X is trapped and less is released during the regeneration event at 465 °C, with an overall 71% NO_X conversion obtained. Further increased performance is observed at 371 °C and there is little difference in NO slip in either the trapping or regeneration phases between the 371 and 286 °C data sets. There are differences in the NO_2 slip between these two operating temperatures, with 286 °C allowing more slip during the latter part of the trapping phase, but less at the beginning. The integrated NO_X conversion achieved over all 30 cycles at 371 °C was 93% and at 286 °C was 94%. At 201 °C, NO slip is observed, with about 1/2 of the entering NO escaping the catalyst at the end of each cycle. Coincident NO_2 slip is observed, most likely due to kinetically limited nitrate formation at this low temperature. The conversion at this temperature over the 30 cycles was 42%. N_2O and NH_3 formation were also tracked but are not presented as part of this study.

During the lean-phase, the catalyst surface traps NO_X and forms nitrates, therefore as time progresses, fewer sites are available for trapping. Once NO_X slip begins, assuming no other influence, this increase in surface nitrate concentration toward saturation would lead to a continuous, monotonic increase in the amount of NO_X escaping the catalyst. However, the data shown in figure 2 indicate that there is not a continuous increase in the escaping NO_2 during the trapping phase at 371 and 465 °C. At 465 °C, for example, the amount of NO_2 exiting the catalyst decreased to approximately 8.5 ppm 10 s after the cycle switched from rich to lean. After another 5 s, the observed NO_2 concentration in the outlet began to increase. The outlet NO_2 amount then went through the expected increasing concentration trend for about 24 s, reaching just above 12 ppm, but then began to decrease. The NO slip data shown in figure 3 are the same as those in figure 1 for the 465 °C test, but with a magnified ordinate scale. The amount of NO observed in the outlet decreased to a minimum value of about 20 ppm 17 s after the rich-phase ended and the trapping phase began. The NO slip then increased for the next 19 s before reaching a local maximum of 32 ppm, and then decreased. The onset of the NO outlet concentration decrease temporally matches that of the NO_2. The 465 °C NO slip data were chosen as they demonstrated the changes more dramatically than the 371 °C test temperature set. The 371 °C temperature data set showed the same local maximum feature; the NO_2 concentration reached 15 ppm and decreased to 12 ppm just prior to the regeneration event and the NO rose from 8 to 15 ppm upon reaching a maximum and then decreasing. Since both NO and NO_2 follow the same trend, it is not an equilibrium shift between the two resulting in a continuously increasing NO_X slip. Therefore, the total NO_X slip increased and then decreased during the trapping phase of the cycle.

Although these shifts in NO_X slip do not appear large, it is quite apparent that there was not the expected continuous increase in NO, NO_2 or total NO_X slip during the trapping phase. This can have a direct impact on operating or control strategies. During the 60-s trapping phase of the test at 463 °C, 3.27 cm^3 of NO

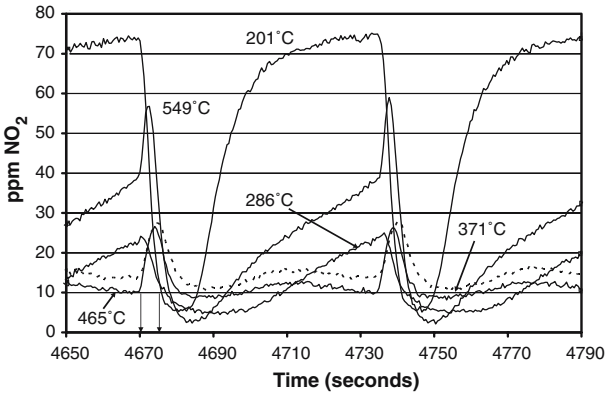

Figure 2. NO_2 outlet concentrations toward the end of a 30-cycle test at 201, 286, 371, 465 and 549 °C. The gas concentrations are listed in the section 2. Arrows at t = 4670 and 4675 s are indicators of the switches to and from the regeneration phase.

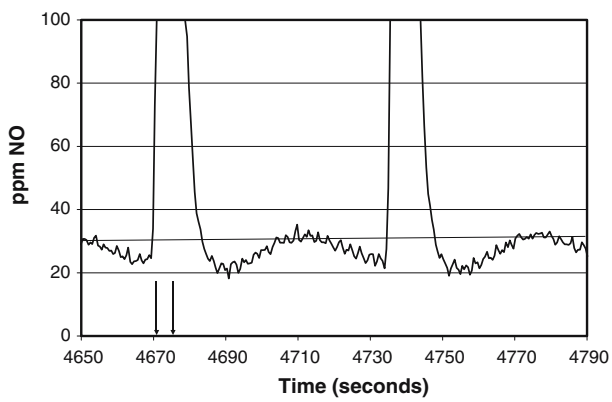

Figure 3. NO outlet concentrations toward the end of a 30-cycle test at 465 °C. These are the same data as shown in figure 1, but expanded in the y-scale. Arrows at t = 4670 and 4675 s are indicators of the switches to and from the regeneration phase.

were input. Of the 3.27cm^3 of NO, 0.35 cm^3 were not trapped. At the peak of NO_X slip, at approximately t = 4710 s on figure 3, 0.23 cm^3 of NO_X had not been trapped, the remaining 0.12 cm^3 slip occurs in the remaining 23 s of the cycle. If, however, the trend in slip would have continued increasing, calculated using a simple linear extrapolation of the slip trend to the regeneration time, an estimated 0.18 cm^3 of NO would not have been trapped during the final 23 s; the increased trapping ability results in an estimated 50% less NO slip after the maximum in outlet concentration was observed. More important is the effect these values would have on a control strategy for NSR catalyst application. If 10% slip is a target for a regeneration event trigger, a NO_X slip value of 30 ppm would cause the controller to implement a regeneration protocol. A regeneration event would have therefore occurred at t = 4706 s for the data presented in figure 3. The lean-phase would have therefore only lasted 32 s. The data shown in figure 3 demonstrate however, that such a trigger is unrealistic, and highly inefficient, since the NO_X slip decreased during the latter portion of the lean-phase. Without accounting for the increased trapping ability after the 32 s, the fuel penalty associated with this operating point would significantly increase. A simple NO_X slip measurement as a control input will therefore not be sufficient, at least in the 370– 465 °C temperature range.

Thermocouple data obtained during the 371 °C nominal target temperature test are shown in figure 4. Before the cycling began the thermocouple positioned just inside a central channel at the inlet face read 366 °C and that positioned inside the channel at the outlet face read 371 °C. The data shown in figure 4 clearly show temperature transients associated with the reductant input. A temperature rise of over 30 °C was observed within the first few millimeters of the catalyst. The temperature rose quickly, reaching the maximum

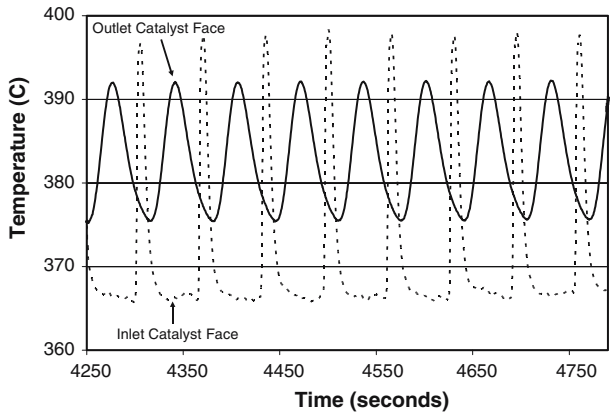

Figure 4. Temperature data obtained in the radial center, just inside the inlet and outlet faces of the catalyst. These data were obtained during the test performed at the nominal operating temperature of 371 °C.

observed at 6.0 s after the regeneration phase began, or 1.0 s after the regeneration event ended and the lean-phase restarted. This temperature then decreased, reaching the nominal inlet temperature approximately 26 s after the lean-phase began. The temperature read just inside the outlet face was both qualitatively and quantitatively different. The temperature rise was less, reaching 392 °C at the maximum. Also, the temperature never decreased back to its initial value of 371 °C, reaching 376 °C at its minimum. Another interesting feature is the reading at the outlet face reached its maximum value 41 s after the regeneration pulse was input, or 36 s after the regeneration pulse ended. At each temperature, even at 193 °C where oxidation rates would be relatively low, the same trends in temperature were observed. The universal exhaust gas oxygen (UEGO) sensor measurements show that at the inlet of the reactor, the time (t90) to reach the input reductant level, the switch from lean to rich, was on the order of 1.5 s while at the outlet of the reactor t90 was achieved after 3 s. Therefore it is not extensive mixing in the reactor causing such phenomena.

As mentioned in the section 1, there are multiple possible sources of a temperature increase. In application, the inlet regeneration/rich-gas may contain some O_2, which combusts with the excess reductant resulting in the generation of an exotherm. Most of the O_2 would be consumed in the front section of catalyst, therefore most of the heat would be generated there as well. The regeneration gas during our tests, however, contained no O_2. A second source of heat would be reaction between reductant and O_2 at the interface between the rich- and lean-phases. Although the reactor is designed to minimize this interaction, it is impossible to eliminate and therefore some mixing is expected. An "inert" interface would be left once both of the components are consumed at this moving mixture interface. It is safely assumed that this would again occur in the front section of catalyst. The same phenomena, albeit possibly to different extents, should be observed with the transition from lean-to-rich and rich-to-lean. This would indicate that if this was a significant effect, two exotherms or temperature increases would be observed per cycle. The data shown in figure 4, however, only contain or demonstrate one "wave" per cycle. Furthermore, this gas-phase interface travels through the catalyst quite quickly relative to the measurement scales, on the order of 0.02 s. A third source of heat is reaction between the reductant and surface oxygen. Pt forms oxide species during the lean-phase [7] and is then hypothetically reduced during the regeneration event. Similarly, oxygen-storage components most likely exist in this catalyst formulation. The reduction of such species, for example ceria, is exothermic and would therefore lead to heat release. How these phenomena, the latter two in this study and all three in real application, are distributed along the catalyst, the extent of each relative to the

others and the competing heat dissipation processes are admittedly not understood at this time. Attempted calculations to associate the heat released via the temperature rise and amounts of reductant burned were confounded by a lack of H_2 measurements during these experiments.

Axial temperature distributions have previously been shown under different operating conditions on a 1″ diameter, 3″ long $Pt/K/Al_2O_3$ NSR catalyst where phosphor thermography data were obtained at different axial locations within a monolith-supported catalyst [10]. The data indicate a similar, sharp increase in temperature, ~60 °C, at the front section of catalyst during a regeneration event. However, under the conditions of that previous test, which actually contained 1% O_2 in the rich-phase with 4% CO, no temperature increase was observed at catalyst positions beyond 1.5″ from the inlet face of the catalyst sample. The $Pt/K/Al_2O_3$ sample has no explicitly added OSC component which may contribute to the lack of continuous temperature rise down the catalyst length. Realize, based on those phosphor thermography data, if measurements would have been obtained upstream and downstream of the catalyst, no temperature changes would have been noted. Even in our current study, the upstream thermocouple changed 0.3 °C from a cycle temperature minimum to maximum, due either to back-diffusion of heat or due to small flow rate differences between the rich and lean-phases, while the downstream thermocouple indicated that the temperature changed 2.2 °C from a cycle minimum to maximum temperature.

Trapping capacity data obtained from this sample are shown in figure 5. The capacities plotted are NO_X trapping capacities calculated from a 15-min lean-phase experiment and again show the typical temperature dependence profile obtained with NSR catalysts. The ability of the catalyst to store NO_X under the test conditions imposed increases until the test temperature reaches 300 °C. The trapping performance of the catalyst under these specific test conditions then decreased and continued to decrease with further temperature increases. In the discussion above, it was noted that the overall NO_X destruction performance did not significantly change between 286 and 371 °C. The data shown in figure 5 however, show a significant loss between these two temperatures. The difference between the experiments of figures 1–4 and figure 5 that results in the apparent discrepancy is the trapping duration. During the 60 s/5 s lean/rich experiments, the incoming NO_X can access a certain number of trapping sites. The amount of NO_X that entered did not approach the saturation amount at the 286 and 371 °C test temperatures, whereas during the 15-min intervals the saturation limit was approached. The 15-min trapping experiment is therefore a more sensitive measure of the temperature dependency. Overall these data demonstrate a greater accessibility of trapping sites at lower temperatures. In analyzing the trapping data presented above (figures 1–3), with the understanding that nitrate stability is a function of temperature, it is apparent that the exotherm-generated temperature increases were affecting the NO_X slip profiles. At the onset of the rich-phase, the temperature at the inlet face of the catalyst increased. It is assumed that along the axial direction relative to flow, the catalyst temperature increased until the reactive surface oxygen was consumed via oxidation of reductant and the gas-phase O_2 was displaced. As the temperature just inside the catalyst increased throughout the regeneration event, there were evidently significant quantities of reactive oxygen species on the catalyst. The generated heat was then either convectively transported or conductively transported. Therefore, even at locations further along the catalyst bed where no more oxygen or reductant remains, a temperature rise can be observed. The thermocouple data as part of this study and the phosphor thermography results from previous work [10] show that the generated heat propagated axially along the catalyst during the regeneration event. Once the regeneration event ended, the catalyst temperature was higher than the entering gas temperature and was not evenly distributed axially. Heat dissipation at the inlet side of the catalyst began, but did not occur at the same rate as the gas-phase travel. Furthermore, some heat was conductively transported along the monolith resulting in an increase in temperature toward the outlet side of the sample well after the regeneration phase had ended. With this relatively slow heat dissipation and conductive transfer down the monolith, the effects of the previous regeneration-induced exotherm were therefore observed well into the trapping phase. Since the nitrate stability increases as the catalyst temperature cools, NO_X slip actually began to decrease late in the trapping phase although there were less sites available for trapping the incoming NO_X. A similar effect was not observed at lower temperatures due to a higher dynamic

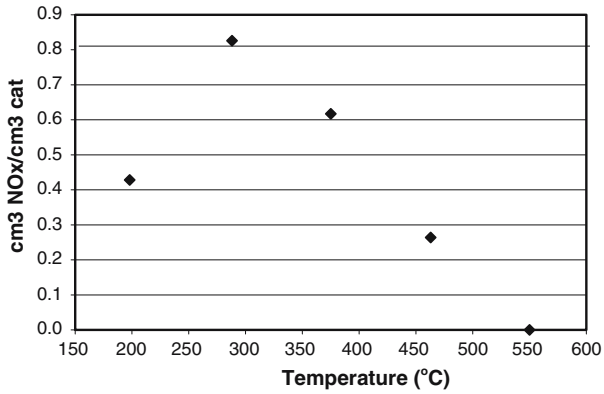

Figure 5. NO_X capacity of the sample as a function of test temperature. These capacities were calculated from sorption experiments where the lean-phase was 15 min in duration – the amount of NO_X on the catalyst approached the sorption capacity for that temperature.

NO_X capacity and nitrate stability, or at a higher temperature due to significantly poorer NO_X trapping efficiency. The observed effects need to be integrated into trapping models and the results also demonstrate the importance of coupling the heat balance into the NSR models. Furthermore, this effect has substantial practical relevance, due to both a need for high integral NO_X trapping efficiencies, and possible use of the instantaneous trapping efficiency as a control strategy feedback trigger.

4. Conclusions

NO_X trapping and nitrate stability are functions of the catalyst temperature. The data obtained in this study demonstrated that the catalyst temperature was not only influenced by the entering gas temperature, but also by any previous exothermic reactions that occurred during the rich-phase regeneration event. In practice, the regeneration phase associated with NSR cycling contains excess reductant relative to O_2. Our results show that even when no O_2 was present in the gas composition of the regeneration phase, the amount of surface oxygen species, on this commercial NSR catalyst, that reacted with the entering reductant was sufficient to cause large increases in measured temperatures in the catalyst channels. The gas-phase temperature measured $\sim$5 mm downstream of the catalyst sample did not reflect the extent of change within the catalyst. With these oxidation reactions, a temperature distribution developed axially. Due to differences in the gas component mass transport, gas-phase heat dissipation and heat conduction through the monolith, a temperature gradient in the catalyst existed and was still evolving many seconds after the exothermic reactions ended. This remaining heat affected the subsequent NO_X trapping efficiency since nitrate stability is a function of catalyst temperature. This leads, under the appropriate conditions, to NO_X slip profiles that do not continuously increase, resulting in multiple relative maxima in outlet NO_X concentrations with exposure time.

References

[1] W.S. Epling, L.E. Campbell, A. Yezerets, N.W. Currier and J.E. Parks II, Catal. Rev. 46 (2004) 163.
[2] E. Fridell, H. Persson, B. Westerberg, L. Olsson and M. Skoglundh, Catal. Lett. 66 (2000) 71.
[3] A. Scotti, I. Nova, E. Tronconi, L. Castoldi, L. Lietti and P. Forzatti, Ind. Eng.Chem. Res. 43 (2004) 4522.
[4] R.L. Muncrief, P. Khanna, K.S. Kabin and M.P. Harold, Catal. Today 98 (2004) 393.
[5] L. Olsson, R.J. Blint and E. Fridell, Ind. Eng. Chem. Res. 44 (2005) 3021.
[6] W.S. Epling, J.E. Parks II, G.C. Campbell, A. Yezerets, N.W. Currier and L.E. Campbell, Catal. Today 96 (2004) 21.
[7] L. Olsson and E. Fridell, J. Catal. 210 (2002) 340.
[8] M. Crocoll, S. Kureti and W. Weisweiler, J. Catal. 229 (2005) 480.
[9] S.S. Mulla, N. Chen, W.N. Delgass, W.S. Epling and F.H. Ribeiro, Catal. Lett. 100 (2005) 267.
[10] J.S. Choi, W.P. Partridge, W.S. Epling, N.W. Currier and T.M. Yonushonis, Catal. Today 114 (2006) 102.